Submarine Floating Antenna Model for LORAN-C Signal Processing

A. MONIN
LAAS-CNRS
France

An electromagnetic model of the floating antenna used by submarines for LORAN-C radionavigation and very low frequency (VLF) communications is proposed. We present a description of the floating antenna and analyze its electric characteristics. The current in the horizontal wire induced by the lateral wave is then computed and we suggest a model that yields to a nonrational transfer function. A parameter estimation algorithm based on parallel-extended Kalman filters is then proposed and validated on real data.

Manuscript received July 30, 2002; revised June 2, 2003; released for publication July 25, 2002.

IEEE Log No. T-AES/39/4/822059.

Refereeing of this contribution was handled by J. A. Tague.

This work was supported by the General Army Direction, France, and the DIGINEXT Company, France.

Author's address: LAAS-CNRS, 7 avenue du Colonel Roche, 31077 Toulouse Cedex 4, France, E-mail: (monin@laas.fr).

I. INTRODUCTION

The antenna used by submarines, for LORAN-C radionavigation and very low frequency (VLF) communications, is made of a long insulated wire ($\cong$ 700 m) dragged by the submarine when it is submerged. A significant part of this wire is located near the surface. For VLF signals, the wave draws into seawater and is picked up by the antenna. The behavior of such an antenna is often reduced, in practice, to a simple model. One generally just considers that the current phase is inverted when the wave path comes from the front to the back of the carrier. Moreover, since the phase center location of the antenna (virtual point where the wave is supposed to be picked up) is not accurately known, the antenna is only used for radio navigation when the incident angle of the path wave with the axis of the antenna is near zero (in practice $\pm 5°$). In order to improve the location accuracy with LORAN-C signal processing, it is necessary to develop a relevant model of such an antenna. To achieve this goal, it is necessary to deal with the electromagnetic properties of these kinds of antenna.

The electric field induced in such an antenna is related to the lateral electromagnetic waves theory (see [1] for a complete bibliography). It may be viewed as a diffraction effect due to the differences between the wave velocity in the air and seawater and may be analyzed using optical Fresnel formula [2]. This kind of wave has been fully studied and the results have been applied to many fields including geophysical exploration, communications, and remote sensing.

The paper is structured as follows. After some electromagnetic preliminaries dealing with the propagation properties of classic electromagnetic waves, we present a physical description of the floating antenna and analyze its electric characteristics. We then evaluate the electric field properties of a vertical dipole transmitting a wave traveling along the boundary between sea and air in reference to the LORAN-C transmitter. Note that these first paragraphs are essentially derived from [1]. We then compute the main current in the horizontal wire induced by the lateral waves. It is shown that the computation of this current is obtained by integration of elementary currents along the axis of the wire. The model involved exhibits a nonrational transfer function between the current induced in the transmitter and the current in the receiver. We then develop a parameter estimation algorithm based on the use of parallel-extended Kalman filters. Finally, the model is validated with real data.

II. ELECTROMAGNETIC PRELIMINARIES

Let us recall that the Fourier transform of the electric field $E(x,t)$ in all homogeneous isotropic

media has the following expression:

$$\hat{E}(\omega,x) = \hat{A}(\omega)e^{-jk(\omega)x}$$
$$k(\omega) = \omega\sqrt{\mu\left(\varepsilon - j\frac{\sigma}{\omega}\right)} \quad (1)$$

where ω stands for the Fourier variable, $k(\omega)$ is the wave number, μ is the permeability, ε is the permittivity, and σ is the conductivity of the medium ($j^2 = -1$). $\hat{A}$ is an integration constant resulting of sources. Performing the inverse Fourier transform, one gets the general solution of the Maxwell equations, that is:

$$E(t,x) = \frac{1}{2\pi}\int_{\mathbb{R}} \hat{A}(\omega)e^{-j(\omega t - k(\omega)x)}d\omega.$$

Let us consider a vertical wire source with current I_t along the axis of the wire. If the wavelength is much smaller than the wire length l, one may assume that the antenna is equivalent to a dipole with electric moment $I_t l$ [3, 4]. When observed in a direction that is orthogonal to the antenna axis, the Fourier transform of the electric field radiated at range ρ, in the far-field region, can be written

$$\hat{E}(\omega,\rho) = -\frac{j\omega\mu_0}{2\pi}\frac{e^{-jk(\omega)\rho}}{\rho}\hat{I}(\omega)l \quad (2)$$

where $\hat{I}(\omega)$ stands for the current Fourier transform. Conversely, for reception, the current induced in a wire antenna of length h by the impressed electric field $\hat{E}(\omega,\rho)$ can be represented by

$$\hat{I}(\omega) = -\frac{2\pi}{j\omega\mu_0}\frac{\hat{E}(\omega,\rho)}{h}. \quad (3)$$

The characteristic impedance of such an antenna, defined by $Z_c = El/I$, is

$$Z_c = -\frac{j\omega\mu_0}{2\pi}.$$

III. FLOATING ANTENNA

A. Description

The floating antenna behavior is described by the theory of lateral electromagnetic waves [1]. The propagation of waves along and across the boundary of two media with different characteristic velocities is illustrated Fig. 1. Suppose that an electromagnetic source is lying on the boundary between air and seawater. Three waves are then generated. In both media, there is a direct wave traveling at velocities depending on their electromagnetic characteristics. In air, this direct wave is the only one that reaches the receiver. In seawater and for frequencies near 100 kHz, as is the case for LORAN-C signal, this direct wave is extremely attenuated. Its power is divided by two after a course of 80 cm long. A third

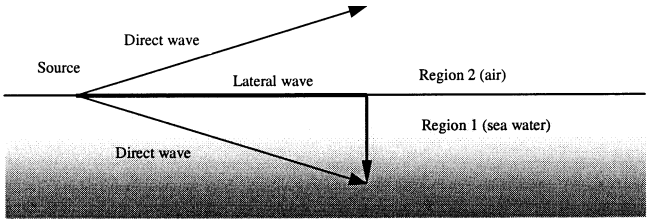

Fig. 1. Lateral electromagnetic wave.

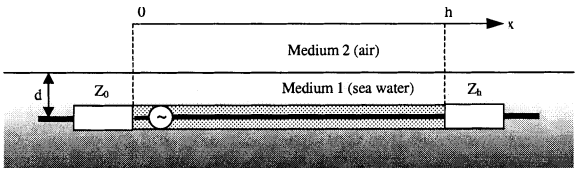

Fig. 2. Floating antenna model.

wave, called lateral wave, travels along the surface of the water in air which continuously generates waves that propagate into the water at the critical angle determined by the ratio of velocities of each medium [2]. This ratio is generally sufficiently great so that the angle of refraction in water is practically 90°. The receiver in the water observes mainly this lateral wave since it travels a long distance in air and then a short distance in water.

The floating antenna used by submarines, for VLF telecommunications and LORAN-C transmitting, consists of a conductor of length h enclosed in an insulating sheath located at a small depth d in seawater [1] (Fig. 2). It is driven at one end against the impedance Z_0 of the receiver. At the other end, the insulated conductor is terminated in second impedance Z_h. Let Z_c be its characteristic impedance. In practice, a maximum current is maintained along the antenna when it is terminated either in a low impedance ($Z_h \ll Z_c$) or in its characteristic impedance ($Z_h = Z_c$).

The current along the insulated horizontal wire is a generalized traveling wave with wave number k_L depending on the antenna properties.

B. Wave Numbers

Let k_1 and k_2 be the waves number of medium 1 and 2, respectively, defined according to (1). In region 1 (air), the medium is lossless and its wave number is defined by

$$k_2 = \omega\sqrt{\varepsilon_0\mu_0} = \frac{\omega}{c} \quad (4)$$

where c is the light velocity in air. In region 2 (seawater), the conductivity of the medium σ_1 is not zero and the wave number has the following regular expression:

$$k_1 = k_2\sqrt{\varepsilon_r - \frac{j\sigma_1}{\varepsilon_0\omega}}. \quad (5)$$

Note that the relative permittivity of seawater ε_r is near 80 when its conductivity is approximately

3.9 S/m. For frequencies near 100 kHz, the ε_r term is negligible in the square root of (5). In fact, $\sigma_1/(\varepsilon_0\omega) \simeq 7.02 \times 10^5$ which is much smaller than 80. Therefore, the wave number in region 1 can be reduced to

$$k_1 = \sqrt{\mu_0\sigma_1}e^{-j\pi/4}\sqrt{\omega}$$

The wave number of the floating antenna has the following general expression [5]:

$$k_L = \sqrt{-z_L y_L}$$

with

$$y_L = \frac{j2\pi k_d^2}{\omega\mu_0 \ln(b/a)}$$

$$z_L = z^i - j\omega\frac{\mu_0}{2\pi}\ln\left(\frac{b}{a}\right) + z^e + z_{12}$$

where $k_d = \omega\sqrt{\mu_0\varepsilon_d}$ is the wave number of the dielectric sheath (outer radius b), a is the radius of the insulated wire, z^i is the internal impedance per unit length, z^e is the series external impedance per unit length and z_{12} is the series mutual impedance per unit length. The expression of z^i can be approximated, depending on the value of $k_c = \sqrt{-j\omega\mu_0\sigma_c}$, the wave number of the conductor:

$$|k_c a| < 2 \Longrightarrow z^i \simeq \frac{1}{\pi a^2 \sigma_c}$$

$$|k_c a| > 5 \Longrightarrow z^i \simeq \frac{jk_c}{2\pi a\sigma_c}.$$

In our case, for copper ($\sigma_c = 5.65 \times 10^7$ S/m), at frequency $f = 100$ kHz and with a conductor radius of 1 mm, one has $|k_c a| = 6.68 > 5$. Consequently, contrary to the case studied in [1], the leading approximation of z^i is

$$z^i \simeq (1-j)\frac{1}{2\pi a}\sqrt{\frac{\omega\mu_0}{\sigma_c}}.$$

In the same way, if $|k_1 b| < 1$ and $|k_1 d| < 1$, z^e and z_{12} can be approximated by

$$z^e \simeq \frac{\omega\mu_0}{4} - \frac{j\omega\mu_0}{2\pi}\left(\ln\left(\frac{2}{k_1 b}\right) - \nu\right)$$

$$z_{12} \simeq \frac{\omega\mu_0}{4} - \frac{j\omega\mu_0}{2\pi}\left(\ln\left(\frac{1}{k_1 d}\right) - \nu\right)$$

with $\nu = 0.5772$. Using all these expressions, the wave number of the insulated antenna is

$$k_L = k_d\sqrt{1 + \frac{1}{\ln\left(\frac{b}{a}\right)}\left(\frac{1}{a\sqrt{\omega\mu_0\sigma_c}} + \ln\left(\frac{2}{|k_1 b|}\right) + \ln\left(\frac{1}{|k_1 d|}\right) - 2\nu + j\left(\frac{1}{a\sqrt{\omega\mu_0\sigma_c}} + \pi\right)\right)}$$

and its characteristic impedance is

$$Z_c = \sqrt{\frac{z_L}{y_L}} = \frac{\omega\mu_0 k_L}{2\pi k_d^2}\ln\left(\frac{b}{a}\right). \tag{6}$$

IV. EVALUATING THE INCIDENT FIELD

The transmitting LORAN-C antenna is equivalent to a vertical dipole in air as described in Section II. The wave travels along the sea surface and acts as a waveguide since its conductivity is not negligible. Therefore, the axial component of the electric field near the boundary of the two media is not quite zero as is the case in homogeneous media. The transverse and axial components of the far field have the following expressions (the subscript is composed of one number related to the region and of one letter, ρ for the axial component and z for the transverse one):

$$\begin{aligned} E_{2_\rho}(\rho) &= -\frac{1}{k_1}F(\rho,k_1,k_2) \\ E_{2_z}(\rho) &= \frac{1}{k_2}G(\rho,k_1,k_2) \end{aligned} \tag{7}$$

where ρ stands for the distance between the source and the receiver. Functions F and G will be defined in the sequel. In water, at depth z, these components are

$$E_{1_\rho}(\rho) = E_{2_\rho}(\rho)e^{-jk_1 z}$$

$$E_{1_z}(\rho) = \frac{k_2^2}{k_1^2}E_{2_z}(\rho)e^{-jk_1 z}.$$

Note that since $k_2^2/k_1^2 \simeq 10^{-6}$ in practice, it is clear that the transverse component in water ($E_{1_z}(\rho)$) is quite negligible with respect to its value in air, as describe in Section I. Conversely, the axial component in sea is the main component of the entire field, only attenuated due to the imaginary part of k_1. Functions F and G are defined by

$$F(\rho,k_1,k_2) = \frac{\omega\mu_0}{2\pi}(f_2(\rho)e^{-jk_2\rho} + f_{21}(\rho)e^{-jk_{21}\rho})$$

$$G(\rho,k_1,k_2) = \frac{\omega\mu_0}{2\pi}(g_2(\rho)e^{-jk_2\rho} + f_{21}(\rho)e^{-jk_{21}\rho})$$

with $f_2(\rho) = -jk_2/\rho - 1/\rho^2$, $g_2(\rho) = jk_2/\rho - 1/\rho^2 + jk_2/\rho^3$, $f_{21}(\rho) = -k_2^3/k_1\sqrt{\pi/(k_2\rho)}\mathcal{F}(k_2^3\rho/(2k_1^2))$ and $k_{21} = k_2(1 - k_2^2/(2k_1^2))$. The function $\mathcal{F}$ is the Fresnel integral defined by

$$\mathcal{F}(u) = \tfrac{1}{2}(1-j) - \int_0^u \frac{e^{-jt}}{\sqrt{2\pi t}}dt.$$

Functions $f_2(\rho)$ (solid line), $g_2(\rho)$ (dashed line) and $f_{21}(\rho)$ (dash-dot line) are shown in Fig. 3. Clearly, for ranges smaller than 5000 km, the magnitude of $f_{21}(\rho)$ is quite negligible with respect to other terms. Moreover, for such ranges, $f_2(\rho) \simeq g_2(\rho)$. Note that for greater frequencies, say such that $k_2\rho \gg |k_1^2|/k_2^2$,

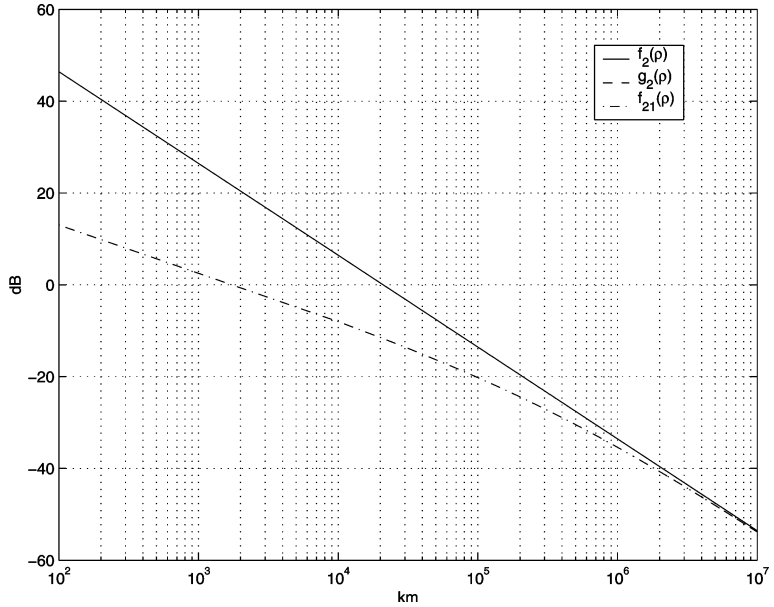

Fig. 3. Variation of attenuation terms with distance from source.

the term $1/\rho^2$ in the expression of $f_2(\rho)$ is dominant since the term $1/\rho$ is canceled by the Fresnel integral. Furthermore, for ranges greater than 10 km, the term $1/\rho^2$ is also negligible with respect to the term $1/\rho$. Finally, for frequencies near 100 kHz and for ranges within 10 km and 5000 km, the actual formula for functions F and G are

$$F(\rho,k_1,k_2) \simeq G(\rho,k_1,k_2) \simeq -\frac{j\omega\mu_0 k_2}{2\pi}\frac{e^{-jk_2\rho}}{\rho}.$$

Using the expression of k_1 in (5), the axial component of the incident electric field in water can be written

$$E_{1\rho}(\rho,z) \simeq -\frac{e^{-j\pi/4}}{2\pi}\frac{\mu_0}{\sqrt{\varepsilon_0\sigma}}\omega^{3/2}\frac{e^{-jk_2\rho}e^{-jk_1 z}}{\rho}. \quad (8)$$

The transverse component in air is

$$E_{2z}(\rho) \simeq -\frac{j\omega\mu_0}{2\pi}\frac{e^{-jk_2\rho}}{\rho}.$$

Note that E_{2z} has the same expression as the electric field radiated by a wire source in a homogeneous medium (2). Finally, the ratio between the transverse component in air and the axial component in water at depth z is

$$\frac{E_{1\rho}(\rho,z)}{E_{2z}(\rho)} = \frac{\sqrt{\omega}}{\sqrt{\varepsilon_0\sigma}}e^{j\pi/4}e^{-jk_1 z}. \quad (9)$$

V. EVALUATING THE RADIATED FIELD

A. Current Along Insulated Wire

Let us define V_0 the electromotive force of the generator. It can be shown that the current is distributed like the one in a generalized transmission line. Its Fourier transform has the following expression:

$$\hat{I}(x) = \frac{j\hat{V}_0}{(Z_0+Z_c)}\frac{\sin(k_L(h-x)-j\theta_h)}{\cos(k_L h - j\theta_h)}$$

where θ_h is the terminal function defined by

$$\theta_h = \coth^{-1}\left(\frac{Z_h}{Z_c}\right). \quad (10)$$

The current in the load Z_0 ($x = 0$) is related to the current at x by

$$\hat{I}(x) = \hat{I}(0)\frac{\sin(k_L(h-x)-j\theta_h)}{\sin(k_L h - j\theta_h)}. \quad (11)$$

The behavior of the antenna depends on the value of the terminal function θ_h:

Matched load: If $Z_h = Z_c$, then $Z_h/Z_c = 1$. According to (10), one has $\theta_h = \infty$. The current behaves like a traveling wave and (11) is simplified as follows:

$$\hat{I}(x) = \hat{I}(0)e^{-jk_L x}. \quad (12)$$

Low-impedance termination: If $Z_h \ll Z_c$, one has

$$\theta_h = r_h + j\left(\frac{\pi}{2} + x_h\right)$$

with $|r_h| \ll 1$ and $|x_h| \ll 1$. In that case, the wave is partially reflected and the current in the antenna becomes

$$\hat{I}(x) = \hat{I}(0)\frac{\cos(k_L(h-x))}{\cos(k_L h)}. \quad (13)$$

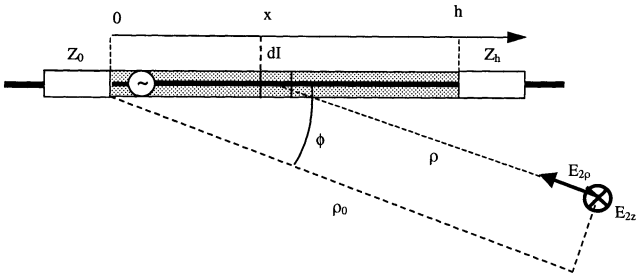

Fig. 4. Top view of antenna.

B. Radiated Field

The antenna may be viewed as a continuous set of dipoles with elementary electric moments $d\hat{I}(x) = \hat{I}(x)dx$.

Let us note ϕ the angle between the propagation direction and the x-axis of the antenna as illustrated Fig. 4. The radial and transverse components of the radiated electric field due to the horizontal dipole $d\hat{I}(x)$ in the sea (medium 1) at distance ρ from the origin are

$$d\hat{E}_{2z}(\omega,\rho,\phi) = \frac{j\omega\mu_0}{2\pi}\frac{k_2}{k_1}\frac{e^{-jk_2\rho}}{\rho}\cos(\phi)d\hat{I}(x)$$

$$d\hat{E}_{2\rho}(\omega,\rho,\phi) = \frac{j\omega\mu_0}{2\pi}\left(\frac{k_2}{k_1}\right)^2\frac{e^{-jk_2\rho}}{\rho}\cos(\phi)d\hat{I}(x)$$

where k_1 and k_2 are defined according to (5) and (4). Note that, with frequency near 100 kHz, one has

$$\left|\frac{k_2}{k_1}\right| = \sqrt{\frac{\varepsilon_0\omega}{\sigma_1}} = 1.19\times 10^{-3}.$$

This leads to consider only the transverse component of the field in the air.

Let ρ_0 be the distance to the receiver referred to the point of reference $x = 0$. Assume that $\rho_0 \gg h$. At distance x from the origin, the distance to the receiver is

$$\rho = \rho_0 - x\cos(\phi).$$

The contribution of the elementary moment $\hat{I}(x)dx$ to the entire field is then:

$$d\hat{E}_{2z}(\omega,x,\phi) = \hat{E}^0_{2z}(\omega,\rho,\phi)e^{jk_2x\cos(\phi)}\frac{\hat{I}(x)}{\hat{I}(0)}dx \quad (14)$$

where $\hat{E}^0_{2z}(\omega,\rho,\phi)$ is the electric field due to an horizontal electric dipole with moment $\hat{I}(0)$ located at $x = 0$, that is:

$$\hat{E}^0_{2z}(\omega,\rho_0,\phi) \triangleq \frac{j\omega\mu_0}{2\pi}\frac{k_2}{k_1}\frac{e^{-jk_2\rho_0}}{\rho_0}\cos(\phi)\hat{I}(0). \quad (15)$$

Let us introduce the effective length of the antenna defined by

$$h_e(\omega,\phi) \triangleq \int_0^h e^{jk_2x\cos(\phi)}\frac{\hat{I}(x)}{\hat{I}(0)}dx.$$

The integration of (14) along the axis of the antenna leads to

$$\hat{E}_{2z}(\omega,\rho,\phi) = h_e(\omega,\phi)\hat{E}^0_{2z}(\omega,\rho_0,\phi) \quad (16)$$

since it is assumed that the amplitude of the incident field is approximately constant over the length h of the wire.

Formula (12) and (13) allow the computation of the effective lengths, that is:

Matched load:

$$h_e(\omega,\phi) = \int_0^h e^{-j(k_L-k_2\cos(\phi))x}dx = \frac{1}{j(k_L-k_2\cos(\phi))}(1-e^{-j(k_L-k_2\cos(\phi))h})$$

Low-impedance termination:

$$h_e(\omega,\phi) = \int_0^h \frac{\cos(k_L(h-x))}{\cos(k_Lh)}e^{jk_2\cos(\phi)x}dx = \frac{1}{(k_L^2-k_2^2\cos^2(\phi))\cos(k_Lh)} \times (jk_2\cos(\phi)(e^{jk_2\cos(\phi)h}-\cos(k_Lh))+k_L\sin(k_Lh)).$$

C. Current in Wire for Reception

Let us consider the LORAN-C transmitting antenna for reception. Let $\hat{E}_{2z}(\omega,\rho,\phi)$ be the incident field defined by (16). According to (3), the current in the load is

$$\hat{I}_r(\omega) = -\frac{2\pi}{j\omega\mu_0 l}\hat{E}_{2z}(\omega,\rho,\phi) \quad (17)$$

where l stands for the receiving antenna length. Using (15)–(17), one has

$$\hat{I}_r(\omega) = -\frac{1}{l}\frac{k_2}{k_1}\frac{e^{-jk_2\rho_0}}{\rho_0}\cos(\phi)h_e(\omega,\phi)\hat{I}(0).$$

Applying the reciprocal theorem to this couple of antennas, if the current in the LORAN-C transmitting antenna is noted $I_e(t)$, the current in the receiving buoyant wire antenna is then:

$$\hat{I}_t(\omega,\phi) = -\frac{1}{l}\frac{k_2}{k_1}\frac{e^{-jk_2\rho_0}}{\rho_0}\cos(\phi)h_e(\omega,\phi)\hat{I}_e(\omega)$$

where

$$I_e(t) = A\left(\frac{t}{t_0}\right)^2 e^{-2((t-t_0)/t_0)}\sin(2\pi f_0 t) \quad (18)$$

with $t_0 = 65$ μs and $f_0 = 100$ kHz.

In conclusion, with (5) and (4), omitting the attenuating factor $1/\rho$ and the pure propagation delay $e^{-jk_2\rho_0}$, the transfer function between the transmitted

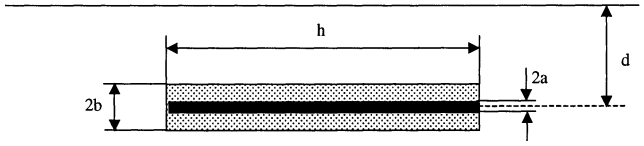

Fig. 5. Insulated antenna.

and received current is:

Matched load:

$$H(\omega,\phi) = -\frac{\sqrt{\omega}e^{-j\pi/4}\cos(\phi)}{(k_L - k_2\cos(\phi))}(1 - e^{-j(k_L - k_2\cos(\phi))h}) \tag{19}$$

Low-impedance termination:

$$H(\omega,\phi) = -\frac{\sqrt{\omega}e^{-j\pi/4}\cos(\phi)}{(k_L^2 - k_2^2\cos^2(\phi))\cos(k_L h)} \times (k_2\cos(\phi)(\cos(k_L h) - e^{jk_2\cos(\phi)h}) + jk_L\sin(k_L h)). \tag{20}$$

Note that these expressions are only defined for $\omega > 0$. As the response of the system is supposed to belong to $\mathbb{R}$, one must have, for all $\omega < 0$, $H(\omega) = H^*(-\omega)$, where H^* stands for the complex conjugate of H. This completes the definition of $H(\omega,\phi)$ for all $\omega \in \mathbb{R}$.

VI. IDENTIFYING THE ANTENNA PARAMETERS

A. Problem Setting

In order to calculate high quality parameter estimates, it is necessary to combine measurements from several transmitter stations or several measurements from a single transmitter. The variables in this context are as follows.

1) Antenna characteristics (see Fig. 5):
   - a: wire radius,
   - b: sheath radius,
   - d: submersion depth,
   - ε_d: dielectric permittivity,
   - h: antenna length,
   - ϕ^k: angle between propagation direction from transmitter k and axis of antenna.
2) A_t^k is the amplitude of the signal from the transmitter $k = 1 \ldots N_s$.
3) τ_t is the amplifier delay.

Concerning the antenna characteristics, in order to reduce the number of parameters, it is convenient to consider a linear approximation of $k_L(\omega)$ near the actual frequency of the signal treated:

$$k_L(\omega) \simeq (n_L - j\alpha_L)\frac{\omega}{c} \tag{21}$$

where n_L may be viewed as the antenna index near the nominal frequency (100 kHz) and α_L as an exponential attenuation coefficient. We have verified that with such an approximation, the distortion induced in the waveform is lower than 1%. Moreover, if the deployed length of the antenna is a parameter which is theoretically known under the operational conditions, the part floating on the surface of water is a priori difficult to determine. Therefore, the working length h is considered as an unknown parameter. The angle ϕ^k is directly computed from $\phi^k = \kappa - \zeta^k - \pi$ where κ stands for the submarine course and ζ^k is the azimuth of the transmitter k.

In short, the state variable to be estimated is reduced to

$$x_t = [A_t^1, \ldots, A_t^{N_s}, \tau_t]^T$$

and the parameters are

$$\theta = [n_L, \alpha_L, h]^T.$$

B. Modeling

The reference signal can be represented in the following way:

$$r(t,\theta,\phi) = \mathcal{F}^{-1}(H(\omega,\theta,\phi)\mathcal{F}(s(t)), \qquad t \in \mathbb{R} \tag{22}$$

where $\mathcal{F}$ stands for the Fourier transform, $s(t)$ is the ideal LORAN-C wave defined by (18) and $H(\omega)$ is the transfer function defined by (19) or (20).

As only one station is observed at each time, it is convenient to consider that the sampled observation process y_t, $t \in \mathbb{N}$ is a vector of $\mathbb{R}^{N_s}$ defined by

$$y_t = \begin{bmatrix} A_t^1 r^1(t\Delta t - \tau_t^1 - \tau_t, \theta) \\ \cdots \\ A_t^n r^n(t\Delta t - \tau_t^n - \tau_t, \theta) \end{bmatrix} + \begin{bmatrix} v_t^1 \\ \cdots \\ v_t^n \end{bmatrix} \triangleq h(t, x_t, \theta) + v_t \tag{23}$$

$$r^k(t,\theta) = r(t\Delta t, \theta, \phi^k)$$

where Δt is the sampling period, v_t stands for the output white noise and τ_t^k is the propagation time delay between the station k and the receiver. It is computed from the GPS data and the station location using the so-called Salt formula [6]:

$$\tau_t^k = \frac{D_t^k}{c} + 2.16 \times 10^{-12} D_t^k + \frac{0.04}{D_t^k} - 4.1 \times 10^{-11}$$

where D_t^k is the geodesic distance from the station k.

Note that we do not take into account here the sky wave interference [7] because we use only stations close to the receiver in the identification procedure ($D \simeq 1000$ km).

As the signal amplitude can fluctuate with time, their variations can be represented by

$$A_{t+1}^k = A_t^k + \delta A_t^k \tag{24}$$

where δA_t^k is a white noise (possibly Gaussian). Similarly, the fluctuation of the amplifier delay is introduced in view to compensate possible errors and variations of GPS location data:

$$\tau_{t+1} = \tau_t + \delta\tau_t \tag{25}$$

where $\delta\tau_t$ is also a Gaussian white noise.

C. Parameter Estimation

The estimation algorithm proposed here uses an approximation of the a posteriori probability density function based on a sample of the parameters to be identified. Let us consider the following discrete time dynamic model:

$$\begin{aligned} x_{t+1} &= f(t,x_t,\theta) + g(t,x_t,\theta)w_t \\ y_t &= h(t,x_t,\theta) + v_t \end{aligned}$$

where x_t is the state vector, θ is a time-invariant vector of parameters, y_t is the output and w_t and v_t are independent Gaussian white noises. If this system is locally linear with respect to x_t, for each value of θ, one can build the extended Kalman filter (EKF) of x_t. Recall that the EKF use is relevant if [8]: 1) the initial uncertainty of the state is small enough compared with the field of linearization validity; 2) the noises have standard deviations small enough to ensure that the standard deviation of the Kalman filter lies on this field of validity.

This leads to the following approximation of the probability density function:

$$p(x_t \mid y_0^t,\theta) \cong \mathcal{G}(x_t;\widehat{x_t(\theta)},P_t(\theta))$$

where $\widehat{x_t(\theta)}$ is the EKF of x_t and $P_t(\theta)$ is its covariance matrix. Here, $\mathcal{G}(x;\bar{x},P)$ stands for the standard Gaussian distribution with mean $\bar{x}$ and covariance P.

Suppose that at time $t-1$, the conditional probability density function for θ is approximated by

$$p(\theta \mid y_0^{t-1}) \cong \sum_{i=1}^{N} \rho_{t-1}^i \delta_{\theta^i}(\theta) \tag{26}$$

where $\delta_{\theta^i}(\theta)$ stands for the Dirac measure centered on θ^i. Using the Bayes rule, one has

$$p(\theta \mid y_0^t) = \frac{1}{\eta} p(y_t \mid y_0^{t-1},\theta) p(\theta \mid y_0^{t-1}) \tag{27}$$

where η is a normalizing constant independent of θ. Replacing $p(\theta \mid y_0^{t-1})$ in (27) by its value defined in (26), one has

$$p(\theta \mid y_0^t) \cong \frac{1}{\eta} \sum_{i=1}^{N} \rho_{t-1}^i p(y_t \mid y_0^{t-1},\theta^i)\delta_{\theta^i}(\theta).$$

Because y_t is supposed to be "almost" Gaussian, one has

$$\begin{aligned} &p(y_t \mid y_0^{t-1},\theta^i) \\ &\quad \cong \mathcal{G}(y_t;h(t,\widehat{x_t(\theta^i)}),H(t,\theta^i,\widehat{x_t(\theta^i)})P_t(\theta^i)H(t,\theta^i,\widehat{x_t(\theta^i)})^T + R) \end{aligned} \tag{28}$$

where $H(t,\theta,x) = (\partial h(t,x,\theta))/\partial x)$ and R is output noise variance. As a consequence, at time t, the conditional probability density function for θ has the following approximation:

$$p(\theta \mid Z_0^t) \cong \sum_{i=1}^{N} \rho_t^i \delta_{\theta^i}(\theta).$$

The normalized weights ρ_t^i are defined recursively using (28):

$$\rho_t^i = \frac{\rho_{t-1}^i p(y_t \mid y_0^{t-1},\theta^i)}{\sum_{i=1}^{N} \rho_{t-1}^i p(y_t \mid y_0^{t-1},\theta^i)}. \tag{29}$$

The minimum variance parameters estimation is then computed using:

$$\hat{\theta} = \sum_{i=1}^{N} \rho_t^i \theta^i \tag{30}$$

and the covariance matrix by

$$P_\theta = \sum_{i=1}^{N} \rho_t^i (\theta^i - \hat{\theta})(\theta^i - \hat{\theta})^T. \tag{31}$$

Recall that this approximation is relevant only if standard deviations $\sqrt{P_t(\theta^i)}$ are sufficiently small with respect to the field of validity of the linearization.

In fact, this filtering procedure can be applied to our case. Indeed, the dynamic model (24), (25) is clearly linear Gaussian and the amplitudes A_t^k appear linearly in the observation model (23). Moreover, the observation model can be linearized with respect to τ_t as long as the standard deviation is low compared with the signal period (10 μs).

The identification is carried out by positioning N samples of θ on a fixed grid. Each one of its nodes represents a set of parameter $\theta^i = [\alpha_L^i, n_L^i, h^i]$. For each sample θ^i, one computes the EKF that estimates the state vector $x_t = [A_t^1,\ldots,A_t^{N_s},\tau_t]^T$ using the following output matrix:

$$H_t(\theta) = \frac{\partial h(t,x_t,\theta)}{\partial x_t}$$

$$= \begin{bmatrix} r^1(t\Delta t - \tau_t^1 - \tau_t,\theta) & \cdots & 0 & -A_t^1 \dfrac{\partial r^1}{\partial t}\Big|_{\tau_t} \\ \cdots & \cdots & \cdots & \cdots \\ 0 & \cdots & r^n(t\Delta t - \tau_t^n - \tau_t,\theta) & -A_t^n \dfrac{\partial r^n}{\partial t}\Big|_{\tau_t} \end{bmatrix}.$$

The identified parameters are then computed using (28), (29), and (30). The evaluation of the standard deviation of the estimate given by (31) is just used to survey the consistency of the identified parameters.

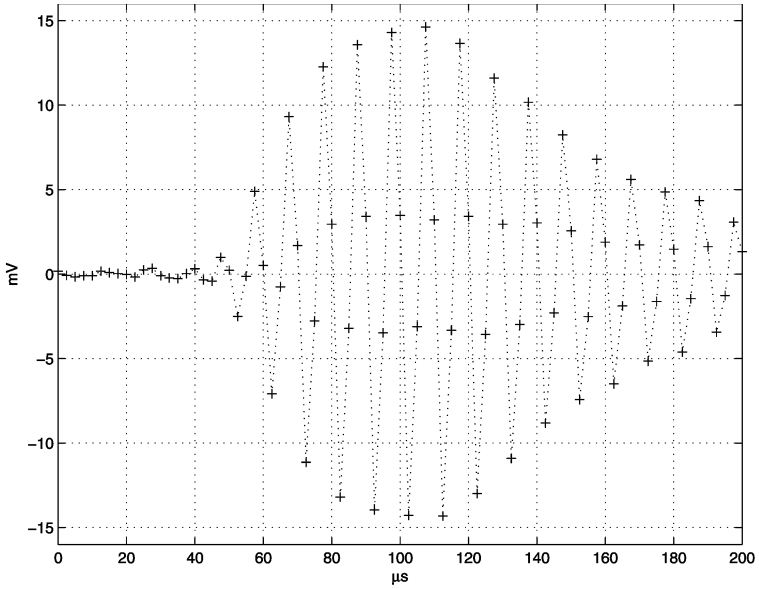

Fig. 6. Signal after summation.

TABLE I
Distances and Incidence Angles

	Record 1	Record 2
Transmitter 1	1090 km/156.1°	1040 km/28.6°
Transmitter 2	975 km/172.2°	930 km/11.6°
Transmitter 3	1225 km/140.2°	1170 km/45.2°

VII. EXPERIMENTAL RESULTS

A. Data Set

We use a set of data that has been collected by a civilian boat freighted by the General Army Direction of France (DGA). The LORAN-C signal was sampled at 400 kHz and time-stamped to a very high accuracy (a few nanoseconds), thanks to the use of a cesium clock. The position reference of the carrier was acquired using a classical GPS receiver. Course and speed are also recorded. The duration of each record is 10 min. The identification had been made using two records for which the transmitters were close to the carrier (distance from transmitters near 1000 km). The distances and incidences of the transmitters used are presented in Table I.

B. Preprocessing

In order to reduce the quantity of calculations necessary to the identification, it is convenient to initially carry out the summation of the samples on a burst of eight pulses, the period of the summation being 1 ms. The signal obtained can then be added up again over several group repetition interval (GRI) periods ($\simeq 0.1$ s). This reduces the signal-to-noise ratio (division of the variance of the additive noise by the number of pulses added up). Note that, as the carrier location is known and the signal dating very accurate, it is possible and appropriate to dismiss all pulses that are supposed to be spoiled by some other LORAN-C transmitter. It should not however be forgotten that, in the calculation, the movement cannot be compensated, which yields to deform the signal. This deformation is connected with an integration of wave for one length of time corresponding to the distance covered during the summation. As an example, for a carrier navigating at 5 mi/h, after 5 s, it traversed approximately 15 m, which corresponds to a time of integration of approximately 0.05 μs. If we compare the starting signal with the integrated one, it is observed that the induced distortion is lower than 0.01%. For these reasons, this duration of summation (5 s) had been appointed. At this stage, each 5 s, we have a pulse at one's disposal which looks like the one shown Fig. 6.

C. Algorithm

Step 1 Sampling the parameter space.

One defines the searching interval for all parameters, that is $[n_{\min}, n_{\max}]$, $[\alpha_{\min}, \alpha_{\max}]$ and $[h_{\min}, h_{\max}]$. A mesh-grid is then constructed with steps defined by

$$\Delta x = \frac{(x_{\max} - x_{\min})}{\sqrt[3]{N}}$$

where N denotes the number of samples used. The standard deviations for τ_t is set to 1 μs ($\ll 10$ μs) making sure the convergence of EKFs. The initial means of $\widehat{A^k}$ are set to their theoretical values computed using [9]. The standard deviations of the amplitudes A^k are set to half of their theoretical values.

TABLE II
Parameters Estimated

Stations	n_L	α_L	h	τ
Transmitter 2	1.35 ± 0.01	0.38 ± 0.01	682 m $\pm$ 6 m	0.17 μs $\pm$ 0.04 μs
Transmitter 1 + 2	1.36 ± 0.01	0.40 ± 0.006	681 m $\pm$ 3 m	0.19 μs $\pm$ 0.03 μs
Transmitter 1 + 2 + 3	1.37 ± 0.01	0.40 ± 0.01	681 $m \pm 2$ m	0.17 μs $\pm$ 0.03 μs
Mean	1.36	0.39	681 m	0.18 μs

TABLE III
Amplitudes Estimated and Their Theoretical Values

Distance	Incidence	Theoretical Attenuation	Amplitude Estimated	Theoretical Value	Difference
940 km	11.6°	−0.41 dB	11.3 mV	11.3 mV	0.0 dB
975 km	180° − 7.8°	−13.1 dB	10.9 mV	10.2 mV	0.5 dB
1045 km	28.6°	−2.5 dB	4.36 mV	5.93 mV	−2.7 dB
1080 km	180° − 9.0°	−13.1 dB	8.98 mV	7.64 mV	1.4 dB
1090 km	180° − 23.9°	−13.4 dB	3.88 mV	5.32 mV	−2.8 dB
1175 km	45.2°	−6.16 dB	7.79 mV	8.10 mV	−0.4 dB
1180 km	180° − 24.1°	−13.4 dB	3.75 mV	4.22 mV	−1.0 dB
1220 km	180° − 39.8°	−14.5 dB	6.22 mV	7.21 mV	1.5 dB
1290 km	180° − 39.4°	−14.5 dB	7.02 mV	6.08 mV	1.2 dB
1135 km	11.7°	−0.42 dB	4.37 mV	4.02 mV	−0.6 dB
1420 km	24.2°	−1.79 dB	1.82 mV	2.28 mV	−2.0 dB
1460 km	10.4°	−0.33 dB	2.09 mV	2.09 mV	0.0 dB
1505 km	37.4°	−4.23 dB	3.31 mV	3.53 mV	−0.6 dB
1530 km	180° − 0.8°	−13.0 dB	2.34 mV	2.45 mV	−0.4 dB
1610 km	11.8°	−0.43 dB	1.35 mV	1.46 mV	−0.7 dB
1620 km	180° − 10.2°	−13.1 dB	1.00 mV	1.43 mV	−1.7 dB
1690 km	180° − 22.0°	−13.4 dB	1.97 mV	2.3 mV	−1.4 dB

Step 2 Reference signals.

For each sample, one calculates the signal of reference as being the result of the filtering of the LORAN-C signal through the defined transfer function (20). The computation is achieved using numerical Fourier transform.

Step 3 Signal summation.

One carries out here the summation of the impulses of the signal, within a GRI, then between GRI as described in subsection B above. The impulses reentering in conflict with others are eliminated on a power criterion. The number of pulses proceeded is collected. The variance of the additive noise divided by this number of summations gives the new variance of noise used by the EKFs. Note that this noise variance can be easily derived by estimating the power of the signal noncontaminated by LORAN-C pulses.

Step 4 Amplifier delay and amplitudes estimation.

The EKFs estimate τ_t and $\{A_t^k\}$, conditionally with the value of the parameters θ^i. The sky wave is not taken into account in this estimate, the studied stations being sufficiently close to the receiver (time of arrival of the sky wave > 65 μs) [7].

Step 5 Weight computation (29).

Step 6 Parameter estimation (30).

Step 7 Convergence test (31).

If the signal-to-noise ratio is such that the estimate has not the accuracy required, one carries out a translation of the point of reference in conformity with dynamics of the carrier (given course and speed) and one turns over in 3. The variances of the Kalman filters are brought up to date in accordance with the prediction errors (variances of $\delta\tau_t$ and δA_t in the dynamic model (25) and (24). Otherwise, the algorithm provides the estimated parameters.

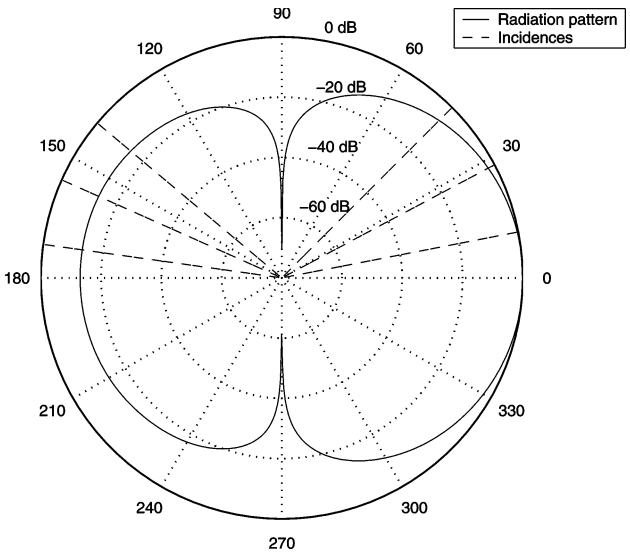

Fig. 7. Radiation pattern.

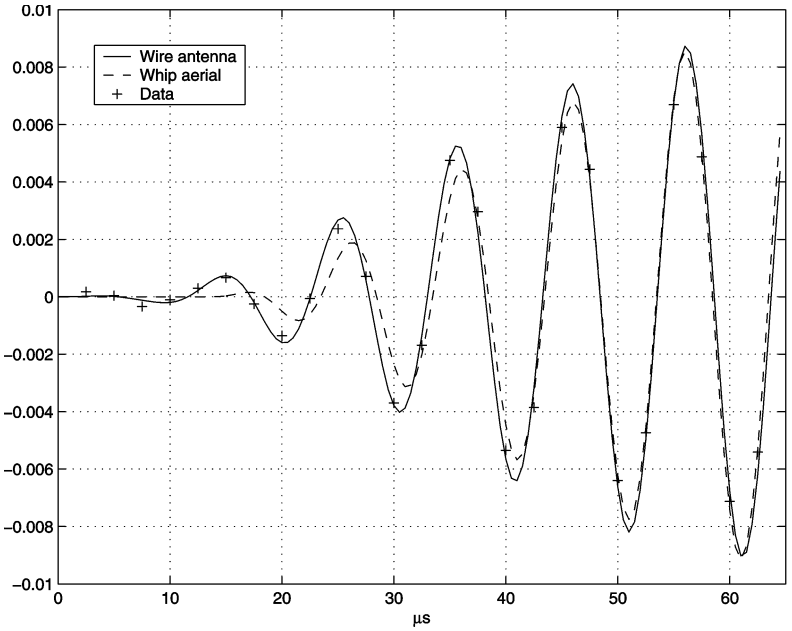

Fig. 8. Comparison wire antenna/whip aerial $\phi = 172°$.

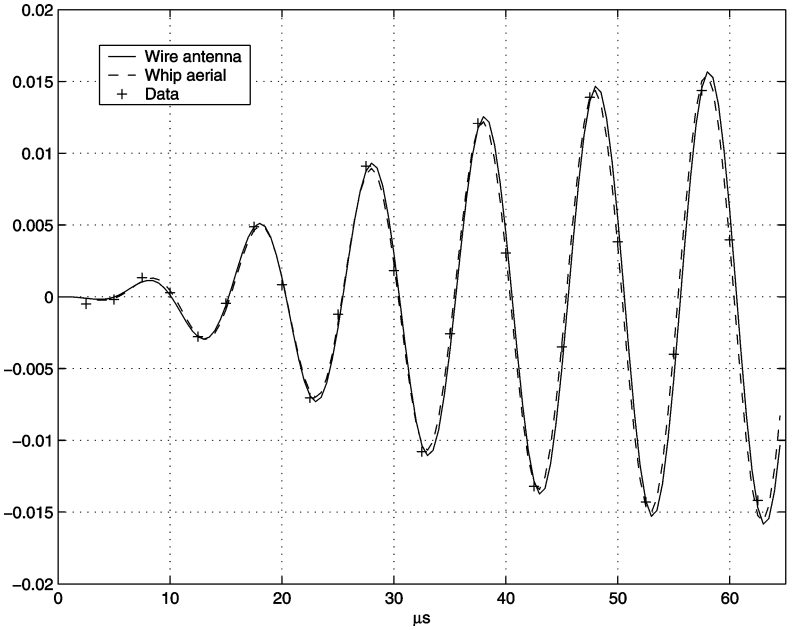

Fig. 9. Comparison wire antenna/whip aerial $\phi = 12°$.

D. Identification

Experimental results have been achieved using data described in Section VIIA. In view to test the algorithm, the parameter estimation algorithm used records 1 and 2 and transmitters 2 (incidences closest to 0° and 180°), 1+2 and 1+2+3. The results are presented in Table II. The induced radiation pattern (computed from (20) at 100 kHz) and the incidences of transmitters used for identification are shown Fig. 7.

In Fig. 8, we show the wave obtained with our identified model for an incidence angle near π (transmitter 2—record 1). It is compared with the wave obtained with the whip aerial model. It appears clearly that our model is able to fit the data with much more accuracy than the whip aerial model does. Note that, however, with this antenna, the error involved in the location is near 3800 m. On the other hand, as shown in Fig. 9, the whip aerial model remains accurate when used with incidence angle near 0 (transmitter 2—record 2). Indeed, the wave deformation induced by the antenna is quite negligible in that case, which explains that this floating antenna is only used in practice in such a situation.

TABLE IV
Propagation Delays Estimated

Distance	Incidence	Floating Antenna	Whip Aerial
940 km	11.6°	−2 m	−23 m
975 km	180° − 7.8°	1 m	3863 m
1175 km	45.2°	−11 m	146 m
1045 km	28.6°	−3 m	67 m
1080 km	180° − 9.0°	33 m	891 m
1335 km	11.7°	−45 m	−65 m
1220 km	180° − 39.8°	−26 m	695 m
1290 km	180° − 39.4°	−36 m	763 m
1090 km	180° − 23.9°	−11 m	3820 m
1180 km	180° − 24.1°	28 m	829 m
1420 km	24.2°	−82 m	−86 m
1460 km	10.4°	8 m	−27 m
1505 km	37.4°	−16 m	−33 m
1530 km	180° − 0.8°	−18 m	818 m
1610 km	11.8°	15 m	−18 m
1690 km	180° − 22.0°	−4 m	775 m
1620 km	180° − 10.2°	−45 m	768 m

VIII. MODEL VALIDATION

A. Radiation Pattern

The magnitude of the current in the wire defined by (20) is theoretically very dependent on the incidence ϕ of the wave, as it appears on Fig. 7. Table III presents the comparison between the magnitude of the signal estimated for some records and their theoretical values computed from [9]. In the third column, the theoretical attenuations at 100 kHz ($\|H(\omega,\phi)\|^2$ with $\omega = 2\pi f_0$) are displayed illustrating variations of the antenna gain for some incidences. In the last column, the difference between the amplitudes estimated and their theoretical values are shown. It turns out that these differences are lower than 2 dB in practice. One may conclude that the radiation pattern produced by our model is close to reality.

B. Positioning Accuracy

Finally, the relevance of our model has been tested by the comparison of the propagation delay estimated with both models (floating antenna and whip aerial). To achieve this goal, we used several records with distances greater than those had been used for identification. The results are presented in Table IV. It appears clearly that the whip aerial model is only relevant for incidences lower than 30° when our model is accurate for all incidences.

IX. CONCLUSION

We have presented a new way for modeling the behavior of the wire antenna used by submarines. The model leads to an important variation of the waveform when used with different incidence angles. It has been shown that the modeled waveforms match real data with a very good accuracy. Moreover, the variations of the antenna gain with the incidences are well treated by such a model. Consequently, it allows extending the use of transmitters with any azimuth, without change of course, as is necessary at the present time. Moreover, one can use several transmitting stations at the same time, which is known to improve the global location accuracy [10, 11].

REFERENCES

[1] King, R. W. P., Owens, M., and Wu, T. T. (1992)
Lateral Electromagnetic Waves—Theory and Applications to Communications, Geophysical Exploration, and Remote Sensing.
New York: Springer-Verlag, 1992.

[2] Andréani-Corbabé, C., Benhabiles-Lacour, B., Depiesse, M., Pellet, M., and Pichot, C. (1998)
Etude d'Antennes sous-marines pour la réception de signaux electromagnétique de très basse fréquence.
Annales des télécommunications, **53**, 7–8 (1998), 835–850.

[3] Balanis, C. A. (1992)
Antenna theory: A review.
Proceedings of the IEEE, **80**, 1 (1992), 7–22.

[4] Thourel, L. (2001)
Antennes À Fil, vol. E3 280, Techniques de l'ingénieur.

[5] King, R. W. P., and Smith, G. S. (1981)
Antennas in Matter: Fundamentals, Theory and Applications.
Cambridge, MA: MIT Press, 1981.

[6] *LORAN-C User Handbook*.
United States Coast Guard, vol. COMDTPUB P16562.6, 1992.

[7] Last, J. D., Farnworth, R. G., and Searle, M. D. (1992)
Effect of skywave interference on the coverage of LORAN-c.
IEE Proceedings, **139**, 4 (1992), 306–314.

[8] Jazwinski, A. H. (1970)
Stochastic Processes and Filtering Theory, Vol. 64.
New York: Academic Press, 1970.

[9] Groundwave propagation curves.
CCIR Record 368-5, vol. 5, 1986.

[10] Monin, A., Rigal, G., and Charron, P. (2000)
A new technology for LORAN-C receivers.
Presented at the International Symposium on Integration of LORAN-C/Eurofix and EGNOS/Galileo, Bonn, Germany, Mar. 2000.

[11] Monin, A., and Salut, G. (2002)
Optimal filtering of LORAN-C signal via particle filtering.
Presented at the EUSIPCO 2002 Conference, Toulouse, France, 2002.

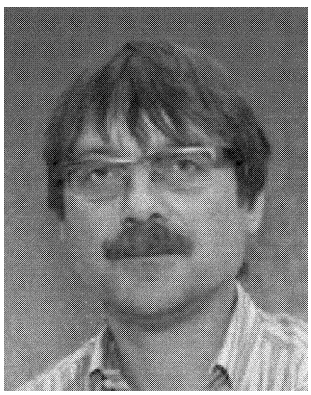

André Monin was born in Le Creusot, France in 1958. He graduated from the Ecole Nationale Supérieure d'Ingénieurs Electriciens de Grenoble in 1980. He obtained the Research Habilitation Thesis in January 2003.

From 1981 to 1983, he was a teaching assistant in the Ecole Normale Supérieure de Marrakech, Morocco. He has been with the LAAS-CNRS (Laboratory for Analysis and Architecture of Systemes of the Scientific Research National Center), France, since 1985, and as a researh fellow since 1989. After some work on nonlinear systems representation for his Doctoral thesis at Université Paul Sabatier, Toulouse, France, in 1987, his interests moved to the area of non linear filtering (specifically Volterra filtering and particle filtering), systems realization and identification (hereditary algorithms under lattice form) applied to GPS, SONAR, LORAN-C, Telecommunications and some other systems.